Evaluating the lateral resolution of the adaptive optics scanning laser ophthalmoscope

Yuhua Zhang
Austin Roorda
University of California, Berkeley
School of Optometry
Room 485, Minor Hall
Berkeley, California 94720-2020
E-mail: yuhuazhang@berkeley.edu

Abstract. We present a statistical assessment of the lateral resolution of the adaptive optics scanning laser ophthalmoscope (AOSLO). We adopt a 2-D Gaussian function to approximate the AOSLO point spread function (PSF), which is dominated by the residual wavefront aberration and characterized by the Strehl ratio. Thus, we derive the lateral resolution in the presence of residual wave aberrations, which is inversely proportional to square root of the Strehl ratio. The modeling, while not sufficient in describing the fine structure of the real PSF, demonstrates good conformance to the lateral cross section of the real PSF. With this model, the lateral resolution of our current AOSLO was computed to be 1.65 to 2.33 μm, which agreed well with the actual result. We also reveal the relationships among the lateral resolution and other three measures of the AOSLO imaging property including the Strehl ratio, the PSF, and the root mean square (rms) of wavefront aberration. [DOI: 10.1117/1.2166434]

Keywords: adaptive optics; scanning laser ophthalmoscopy; point spread function; resolution.

Paper 05066RR received Mar. 10, 2005; revised manuscript received Sep. 15, 2005; accepted for publication Sep. 24, 2005; published online Jan. 25, 2006.

1 Introduction

The adaptive optics scanning laser ophthalmoscope (AOSLO) was demonstrated to produce *in vivo* microscopic views of the living human retina with unprecedented resolution[1] and has emerged as an attractive microscopic imaging modality with promise to improve diagnosis, understanding, and even treatment of blinding retinal diseases. Appropriately assessing the lateral optical resolution of the AOSLO is significant in system performance evaluation and system design as well as optimization.[2] For instance, it can help us to specify a tolerable degradation factor of the system performance so that we can subsequently define a reasonable error budget. It can also help us to reasonably characterize an optimal system bandwidth for AOSLO imaging signal conditioning and processing.

Fundamentally, a scanning laser ophthalmoscope (SLO) is a confocal scanning laser microscope. If it had an ideal objective lens, it should have a better lateral resolution by 27% than a conventional microscopic imaging system with equal objective-lens pupils, a fact that was very well treated by Wilson and Sheppard,[3] Sheppard and Shotton,[4] Webb et al., and Webb.[5,6] But the fact is that the SLO must employ the human eye as its objective lens, whose optical quality is unfortunately far from a diffraction-limited state, especially for large pupils. As a result, the point spread function (PSF) of the SLO, instead of being a sharp Airy disk spot, is a complex speckle pattern that is dominated by the eye's wave aberration, pupil size, etc.[7–12] Moreover, the aberrations and the corresponding PSFs are different and unique for each individual eye. Thus, the SLO performs with varying system aberrations and gives different PSFs. In this situation, it is difficult to give a decent definition and measurement of the PSF for an SLO (Ref. 12). Consequently, considering the aberrations of the eye's optical system, it is nearly impossible to properly assess the real resolution and objectively estimate the limits of SLO imaging quality.

With adaptive optics (AO) correction, the PSF, which is originally dispersed randomly and severely, is forced to concentrate to an approximately Gaussian image point. Although AO correction varies between individual eyes, the root mean square (rms) of the aberration can be statistically compensated to quite a low level. It becomes feasible to evaluate the lateral resolution via mathematical modeling of the PSF, and this is the goal of this paper.

Our paper starts with an analysis of the PSF formation of the AOSLO, which depends on the fact that the static AOSLO images are typically generated from multiple-frame image registration and averaging. Given that a summed frame is a combination of the same image blurred by many instances of a variable PSF, we assume a 2-D Gaussian function to describe the light intensity distribution of the AOSLO real PSF. Thus, we build a statistical PSF model that depends on the presence of residual wavefront aberration, from which we derive the real resolution of the AOSLO. Finally, we assess the PSF models and the lateral resolution with actual AOSLO imaging. The paper will also reveal relationships among four measures describing the AOSLO imaging performance,

Address all correspondence to Yuhua Zhang, University of California, Berkeley, School of Optometry, Room 485, Minor Hall, Berkeley, California 94720-2020. Tel.: (510)643–9396; Fax: (510)643–5109; E-mail: yuhuazhang@berkeley.edu

1083-3668/2006/11(1)/014002/5/$22.00 © 2006 SPIE

namely, the rms of wavefront aberration, the Strehl ratio, the PSF, and the lateral resolution.

2 Method

2.1 *Ideal Lateral Resolution of the AOSLO*

The PSF of the AOSLO is formed by a double-pass reflection in the human eye.[13,14] This process is essentially the same as that of a confocal scanning microscope, which was well expounded by Wilson and Sheppard.[3] Ideally, if (1) the SLO intermediate optical system was very well constructed, (2) the human eye was a perfect diffraction-limited optical system, and (3) we used a pinhole of infinite small size (a point pinhole), the AOSLO PSF would be[3]

$$I(v) = I_0[2J_1(v)/v]^4, \tag{1}$$

where I_0 is the peak intensity of the image of a point object; $J_1(v)$ is the first-order Bessel function; and v is the optical coordinate and is related to the real-space polar coordinate r on the retina plane, via

$$v \approx 2\pi ar/\lambda f, \tag{2}$$

where a is the radius of the eye's pupil, f is the focal length of the eye, and λ is the laser wavelength in the eye, which is a quotient of the laser wavelength in air over the eye's index of refraction.

The ideal lateral resolution can be measured by the full width at half maximum intensity (FWHM) of the PSF. Calculating the value of v_d at which the intensity falls to one half of its value at $v=0$, we obtain the ideal lateral resolution $2v_d$ at the retina.

$$2v_d = 2.32. \tag{3}$$

However, Sheppard and Shotton[4] and Wilson[15] pointed out that this resolution would quickly deteriorate to that of conventional microscopes with enlarging pinhole size. To take advantage of the superior lateral resolution from the confocal configuration, we should have a pinhole size with dimension $v \leqslant 0.5$, which leads to the optimal pinhole diameter that is much smaller than the Airy disk that is formed by the collection lens. This is hard to adopt in the AOSLO because the human retina only reflects, on average, about 1 of 10,000 incident photons.[16] Furthermore, given that our incident exposures are limited by laser safety thresholds for the human eye, the signal photons are too sparse and too precious to lose. We must compromise to a relatively large pinhole size to collect enough photons for imaging. If the pinhole size is sufficiently large, we may treat the AOSLO as a conventional microscope. Under this situation, the PSF will be

$$I(v) = I_0[2J_1(v)/v]^2, \tag{4}$$

which leads to an ideal resolvable distance at the retina

$$2v_d = 3.24. \tag{5}$$

Thus, allowing for a practical size of the pinhole that is larger than the optimal one, the AOSLO lateral resolution will be most likely within the region that is defined by Eqs. (3) and (5).

Note that an AOSLO using a large pinhole may not be able to take advantage of enhanced lateral resolution via the confocal mechanism. But its depth discrimination ability is much more forgiving to the enlarged pinhole. Although a relatively large pinhole compared with that required for improving lateral resolution is adopted, a satisfactory axial sectioning performance is still attainable.[4,14,15]

2.2 *Approximation of the Real AOSLO PSF with the Gaussian Function*

Distinctly, from Fig. 1 without AO correction, the PSF is highly scattered and it is difficult to assess the actual resolution. After wave aberration compensation, the PSF becomes well concentrated, making it feasible to define the resolution mathematically.

To generate a decent static AOSLO image, we first do multiple-frame image registration to correct the image translation that is caused by translational eye movements, and then we select and average many frames to eliminate the imaging noise. In the image, each pixel actually appears with its statistical expectation brightness. So, we assume a 2-D Gaussian function to approximate the light intensity distribution of the PSF. When the system is aberration-free, the PSF takes the form

$$I(\rho,\sigma) = I_0 \exp(-\pi\rho^2). \tag{6}$$

This Gaussian function centers at the origin point and has a variance σ that equals $1/(2\pi)^{1/2}$; ρ is a normalized polar coordinate, and I_0 represents the peak intensity of the diffraction-limited image spot. With aberration this is broadened to[17]

$$I(\rho,\sigma) = \frac{1}{2\pi\sigma^2} I_0 \exp\left(-\frac{\rho^2}{2\sigma^2}\right). \tag{7}$$

The $1/(2\pi\sigma^2)$ is required to conserve energy so that $\int\int I(\rho,\sigma)\rho\, d\rho\, d\theta = I_0$ and is equal to the Strehl ratio S_R. Thus, we get an equation that links the PSF and the Strehl ratio:

$$I(\rho,S_R) = S_R I_0 \exp(-\pi S_R \rho^2). \tag{8}$$

The next step is to relate the normalized polar coordinate ρ to real space. Expanding the diffraction-limited PSF, i.e., Eqs. (1) and (4), as a power series in ν and matching up ν^2 with a Gaussian function,[18,19] we obtain, for the ideal point pinhole case:

$$I(v) \approx I_0 \exp(0.5\nu^2). \tag{9}$$

And, for a large pinhole,

$$I(v) \approx I_0 \exp(0.25\nu^2). \tag{10}$$

Comparing with Eq. (6), we have, for a confocal point size pinhole,

$$\pi\rho^2 = 0.5\nu^2, \tag{11}$$

and for a large pinhole,

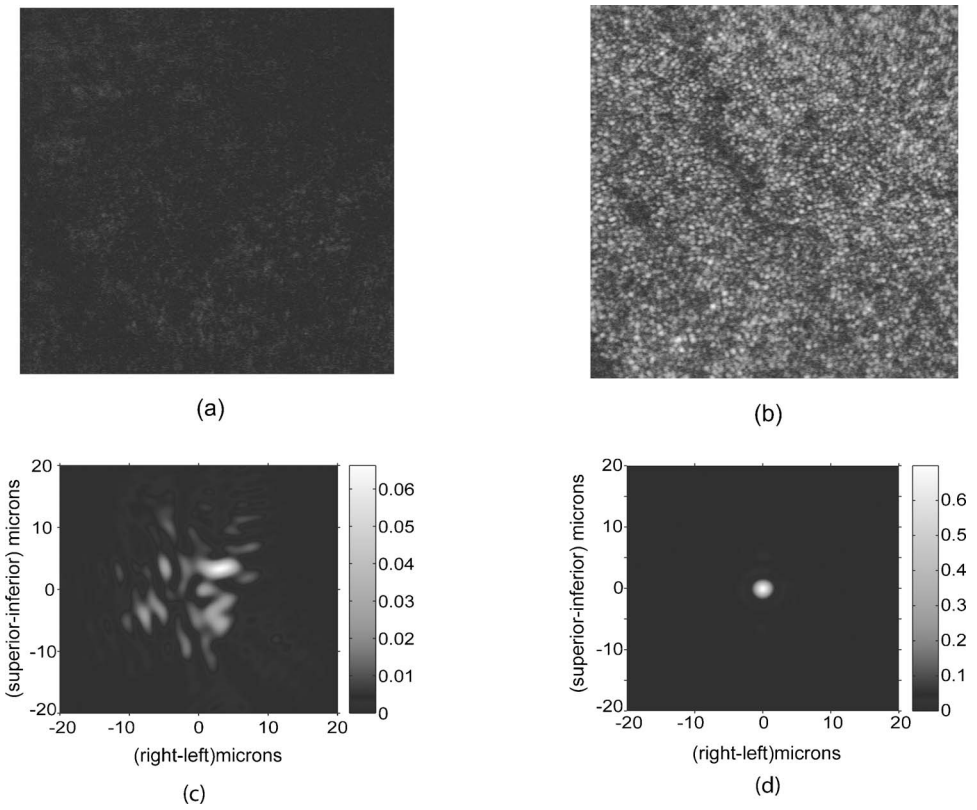

Fig. 1 (a) and (b) AOSLO images of the same area of retina taken without and with AO aberration correction, respectively. These images are of a 1 deg field of view (about 300 microns). The images were taken in an region about 1 deg from the central fovea and averaged 20 frames of the registrated ones. The mosaic of bright features are the cone photoreceptors, which, at this location in the retina, are separated by about 5 μm. The dark lines are shadows of the capillaries, which are anterior to the confocal image plane. (c) PSF corresponding to image (a) in which the eye's rms wave aberration is about 0.64 waves, whereas (d) PSF corresponding to image (b) in which the rms wavefront aberration was decreased to 0.09 waves. The wavefront was measured over a 3-mm radius pupil by the Shack-Hartmann wavefront sensor of the AOSLO.

$$\pi\rho^2 = 0.25\nu^2. \tag{12}$$

Putting $\pi\rho^2$ back to Eq. (8), we obtain the real PSF for ideal point pinhole case:

$$I(v, S_R) = S_R I_0 \exp(-0.5 S_R \nu^2), \tag{13}$$

and for the case of a large pinhole:

$$I(v, S_R) = S_R I_0 \exp(-0.25 S_R \nu^2). \tag{14}$$

When $S_R = 1$, we calculate the PSF difference between Eq. (13) and Eq. (1), which results in a maximum relative error is as low as 2.4% of the peak intensity, as shown in Fig. 2(a). For the difference between Eq. (14) and Eq. (4), the maximum relative error is 5.5% of the peak intensity, as shown in Fig. 2(b). The models conform to the PSF shapes very well.

2.3 *AOSLO Real Lateral Resolution*

Calculating the PSF FWHMs from Eqs. (13) and (14), we acquire the AOSLO resolution $2v_{rd}$ when ocular aberrations are present. With an ideal point-sized pinhole,

$$2v_{rd} = 2.36/\sqrt{S_R}, \tag{15}$$

while for a large pinhole,

$$2v_{rd} = 3.34/\sqrt{S_R}. \tag{16}$$

Normalizing Eqs. (15) and (16) with their corresponding diffraction-limited resolution values, we obtain a general expression of the AOSLO real resolution:

$$r_n \approx 1/\sqrt{S_R}. \tag{17}$$

2.4 *Assessing the AOSLO Resolution*

The laser wavelength of the AOSLO (then at the University of Houston) was 0.660 μm. The eye was dilated and the pupil radius was 3 mm. The eye's focal length and refractive index, taken from the Gullstrand-LeGrand model eye, are 22.27 mm and 1.337, respectively. Statistically, after the AO correction, the residual aberration was lower than 0.1 wave. For the example case demonstrated in Fig. 1, before AO correction, the Strehl ratio was measured to be about 0.015. When AO was turned on, the measured Strehl ratio increased to 0.70. From Eqs. (15) and (16), the lateral resolution of Fig. 1(b) is estimated to be between 1.65 and 2.33 μm. Figure 3(a) shows the real PSF, which is an average of a series of PSFs that were computed from continuous recordings of the wave aberrations that remained after best AO correction. Figure 3(b) shows the PSF cross sections, which are indicated in Fig. 3(a) along with

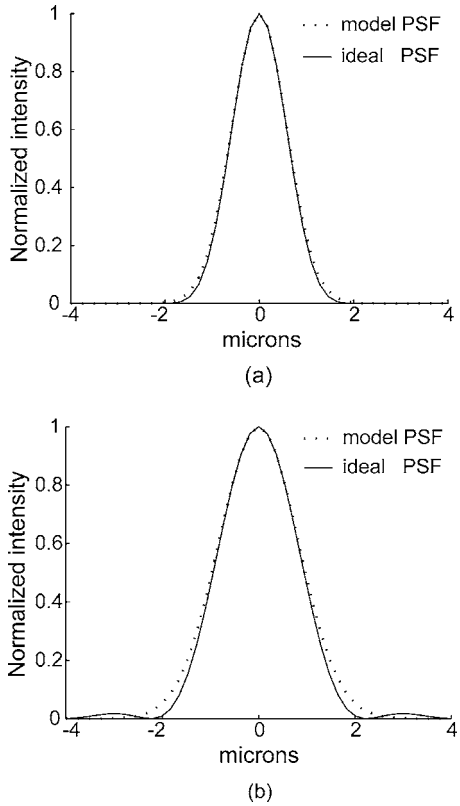

Fig. 2 PSF modeling errors.

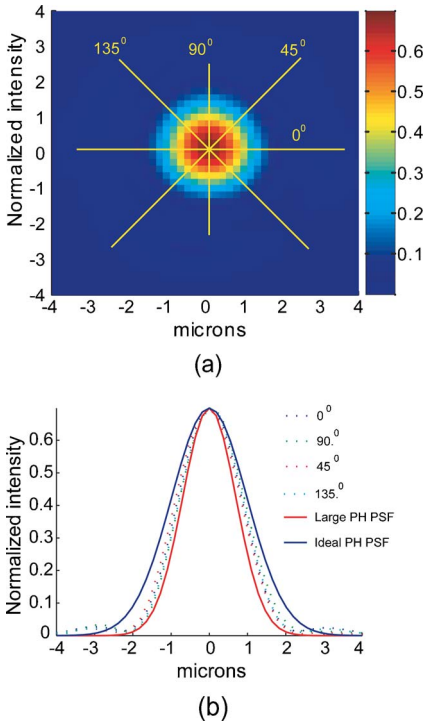

Fig. 3 AOSLO real PSF and modeling errors.

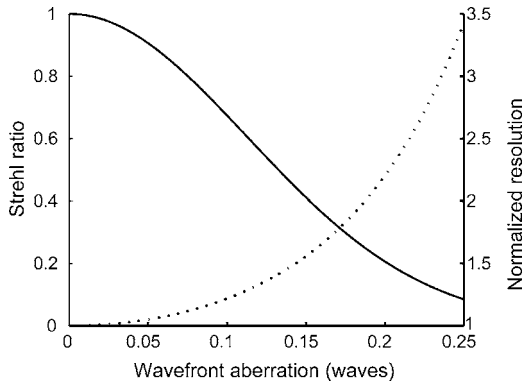

Fig. 4 Strehl ratio as a function of rms wave aberration (solid curve) and the normalized lateral resolution varying with the rms wave aberration (dashed curve).

the PSF models of Eqs. (13) and (14). This demonstrates good agreement between the estimation and measurement. It also agrees well with the images in Fig. 1. Although absolute resolution levels are difficult to assess with an image, the AO-corrected image does show a well-resolved cone mosaic.

Figure 3 also serves as a further evaluation of the PSF modeling accuracy. The models maintain good conformance to the lateral cross section of the real PSF. The maximum relative error for the large-pinhole model is 19.5% of the peak intensity. For the point-pinhole model, this error is 18.4%. Note that the real PSF is not symmetric, and that the model is not sufficient in describing the sidelobes and the asymmetric local structure of the PSF.

3 Discussion

We derived relationships between the primary metrics that define optical quality in the AOSLO imaging system. To apply the formulas, the Strehl ratio for Eqs. (15) and (16) could be obtained from a real measurement, but that proves difficult in the human eye. The PSF and resolution are also difficult to assess from real data. In fact, the simplest metric to directly measure during imaging is the wave aberration. After AO correction, the Strehl ratio is generally greater than 0.1, so we may simply relate the Strehl ratio to the rms of the residual wavefront aberration.[20] Therefore, given the rms of the wave aberration, we can calculate the Strehl ratio and lateral resolution and approximate the PSF. Figure 4 plots these relationships.

4 Conclusion

We derived an objective assessment of the real lateral resolution of the AOSLO imaging via a statistical Gaussian PSF model. The resolution and PSF models supply a set of quantitative relationships for the design, optimization, and evaluation of the AOSLO. But, based on the Gaussian approximation, the PSF model is unable to describe the fine structure of the real PSF. So while the model may predict resolution, it is not recommended for image postprocessing such as deconvolution in restoring image quality.

Acknowledgments

This work is funded by a National Institutes of Health (NIH) Bioengineering Research Partnership, Grant No. EY014365, and the National Science Foundation Science and Technology Center for Adaptive Optics, managed by the University of California, Santa Cruz, under cooperative agreement No. AST-9876783. We also gratefully acknowledge the reviewers' comments and advice on this manuscript.

References

1. A. Roorda, F. Romero-Borja, W. J. Donnelly, III, H. Queener, and T. J. Hebert, and M. C. W. Campbell, "Adaptive optics scanning laser ophthalmoscopy," *Opt. Express* **10**, 405–412 (2002).
2. R. R. Parenti, "System design and optimization," Chap. 2 in *Adaptive Optics Engineering Handbook*, R. K. Tyson, Ed., pp. 29–58, Marcel Dekker, New York (2000).
3. T. Wilson and C. J. R. Sheppard, *Theory and Practice of Scanning Optical Microscopy*, Academic Press, London (1984).
4. C. J. R. Sheppard and D. M. Shotton, *Confocal Laser Scanning Microscopy*, Springer-Verlag, New York (1997).
5. R. H. Webb, G. W. Hughes, and F. C. Delori, "Confocal scanning laser ophthalmoscope," *Appl. Opt.* **26**, 1492–1499 (1987).
6. R. H. Webb, "Confocal optical microscopy," *Reports Progr. Phys.* **59**, 427–471 (1996).
7. A. Roorda, "A review of basic wavefront optics," Chap. 2 in *Wavefront Customized Visual Correction*, R. R. Krueger, R. A. Applegate, and S. M. MacRae, Eds., pp. 9–17, SLACK Inc., Thorofare, NJ (2004).
8. J. Liang and D. R. Williams, "Aberrations and retina image quality of the normal human eye," *J. Opt. Soc. Am. A* **14**, 3873–2883 (1997).
9. J. Porter, A. Guirao, I. G. Cox, and D. R. Williams, "Monochromatic aberrations of the human eye in a large population," *J. Opt. Soc. Am. A* **18**, 1793–1803 (2001).
10. J. Liang, D. R. Williams, and D. T. Miller, "Supernormal vision and high-resolution retinal imaging through adaptive optics," *J. Opt. Soc. Am. A* **14**, 2884–2892 (1997).
11. D. R. Williams, J. Liang, D. T. Miller, and A. Roorda, "Wavefront sensing and compensation for the human eye," Chap. 10 in *Adaptive Optics Engineering Handbook*, R. K. Tyson, Ed., pp. 287–310, Marcel Dekker, New York (2000).
12. W. J. Donnelly III and A. Roorda, "Optimal pupil size in the human eye for axial resolution," *J. Opt. Soc. Am. A* **20**, 2884–2892 (2003).
13. A. Roorda, "Double pass reflections in the human eye," PhD Dissertation, University of Waterloo, Canada (1996).
14. K. Venkateswaran, F. Romero-Borja, and A. Roorda, "Theoretical modeling and evaluation of the axial resolution of the adaptive optics scanning laser ophthalmoscope," *J. Biomed. Opt.* **9** (1), 132–138 (2004).
15. T. Wilson, "The role of the pinhole in confocal imaging systems," Chap. 11 in *The Handbook of Biological Confocal Microscopy*, 2nd. ed., J. B. Pawley, Ed., pp. 167–182, Plenum, New York (1995).
16. F. C. Delori and K. P. Pflibsen, "Spectral reflectance of the human ocular fundus," *Appl. Opt.* **28** (6), 1061–1077 (1989).
17. Y. Zhang, J. Yan, and D. Zhao, "Evaluating the real resolution of optical system by Strehl ratio," *Opt. Tech.* **5**, 1–6 (1999).
18. C. J. R. Sheppard, "Imaging formation in three-photon fluorescence microscopy," *Bioimaging* **4**, 124–128 (1996).
19. C. J. R. Sheppard and T. Wilson, "The theory of scanning microscopes with Gaussian pupil functions," *J. Microsc.* **114**, 179–197 (1978).
20. J. C. Wyant and K. Creath, "Basic wavefront aberration theory for optical metrology," Chap. 1 in *Applied Optics and Optical Engineering*, Vol. **XI**, R. R. Shannon and J. C. Wyant, Eds., pp. 1–53, Academic Press, San Diego, CA (1992).